A Ponderomotive Guiding Center Particle-in-Cell Code for Efficient Modeling of Laser–Plasma Interactions

Daniel F. Gordon, W. B. Mori, and Thomas M. Antonsen, Jr., *Member, IEEE*

***Abstract*—A novel particle simulation code is described that self-consistently models certain classes of laser–plasma interactions without resolving the optical cycles of the laser. This is accomplished by separating the electromagnetic field into a laser component and a wake component. Although the wake component is treated as in a fully explicit particle-in-cell (PIC) code, the laser component is treated in the high-frequency limit, which allows the optical cycles to be averaged out. This leads to enormous reductions in computer time when the laser frequency is much greater than all other frequencies of interest.**

This work is an extension of the work of Mora and Antonsen, Jr. [1], [2], who derived the time-averaged equations coupling the laser with the particles and developed a code to solve these equations in the quasi-static limit. The code presented here is distinguished by the fact that it is useful when the plasma length is much less than the laser pulse length. Also, it is already parallelized and should be straightforward to extend to three dimensions.

***Index Terms*—Particle code, plasma simulation.**

I. Introduction

THE physics of nonlinear laser–plasma interactions is directly relevant to a number of applications, including laser fusion [3]–[5], plasma based accelerators [6], and advanced radiation sources [7], [8]. The complexity of these systems has led many researchers to make heavy use of computer modeling to predict their behavior. The most accurate of such models is probably the particle-in-cell, or "PIC" code. A PIC code self-consistently calculates the motions of a large number of charged particles and the fields they produce. The drawback of such a code is that it requires enormous computing resources to run. This problem becomes particularly acute with regard to laser–plasma interactions because resolving the high-frequency laser field requires a large number of simulation cycles.

Various attempts to overcome this difficulty have been made. The simplest was to prescribe a nonevolving laser field and superimpose its ponderomotive force over the self-consistent force on a particle [9]. Because the ponderomotive force varies slowly on the timescale of the laser frequency (ω_0), only the plasma frequency (ω_p) had to be resolved and an $(\omega_0/\omega_p)^2$-fold increase in the speed of the simulation was obtained. The problem with this approach is that the laser radiation is not allowed to evolve. Processes such as self-focusing and stimulated Raman scattering (SRS) are therefore excluded from the model.

A more sophisticated solution, from Mora and Antonsen, Jr. [2], was to derive a self-consistent description of the interaction between the particles and the laser field in terms of only the slowly varying laser envelope and the associated ponderomotive force. In this way, a factor $(\omega_0/\omega_p)^2$ performance increase was obtained while still allowing the laser pulse to evolve. The code, called WAKE, has been successfully used to model the self-modulation and self-focusing of an intense laser pulse in a plasma. Some of the limitations of WAKE are as follows. First, it uses the quasi-static approximation [10] to solve for the particle motions and the plasma fields. This implies that high-energy particles may not be modeled accurately. Second, because the model equations were expressed in terms of laser coordinates $(\xi = t - x/c, \tau = t)$, the code automatically does all of its calculations in a window moving with the laser pulse. Although this is exactly what is desired in some cases, it is not desirable in others. Finally, because of the structure of the code, it is difficult to parallelize.

In this paper, we describe a new parallel code called turboWAVE that solves Maxwell's equations for the plasma fields and the Mora and Antonsen, Jr. equations for the laser fields. The turboWAVE algorithm is based largely on the Los Alamos code WAVE [11], which has been well tested over the years. Although turboWAVE and WAVE are close algorithmically, programatically turboWAVE is an entirely new object-oriented C++ code.

The distinction between turboWAVE and WAKE can be understood as follows. In both codes, the cell size must be small enough to resolve the nonlinear wake. In turboWAVE, this implies that the timestep must be small enough to resolve a plasma period in order to satisfy the Courant condition. In WAKE, on the other hand, the quasi-static assumption is made and only the laser evolution time needs to be resolved. However, the box size has to be larger than the laser pulse length because the calculation is done in the laser frame. By contrast, turboWAVE allows a laser to be injected into a stationary box that is much shorter than the laser. This is advantageous, for example, when modeling beatwave acceleration experiments. In addition, the removal of the quasi-static approximation allows turboWAVE to model the acceleration of charged particles to high energies,

Manuscript received January 20, 2000; revised February 9, 2000. This work was supported by NSF, under Grant DMS-9722121, and DOE, under Grant DE-FG03–92–ER40727.

D. F. Gordon is with the Naval Research Laboratory, Washington, DC 20375 USA.

W. B. Mori is with the Department of Electrical Engineering and the Department of Physics and Astronomy, University of California at Los Angeles, Los Angeles, CA 90095 USA.

T. M. Antonsen, Jr., is with the Institute for Plasma Research, University of Maryland, College Park, MD 20742 USA.

Publisher Item Identifier S 0093-3813(00)07238-6.

provided the accelerated particles are not affected too strongly by the laser fields.

At present, turboWAVE has the following features and limitations.

1) It solves for high-frequency fields and their effects on particles using a time-averaged model that can lead to much shorter simulation times than those obtained using an ordinary PIC code.
2) In terms of push time per particle per timestep, it runs roughly a factor of two slower than other PIC codes because of the complexity of the algorithm.
3) It functions as a fully explicit two-dimensional (2-D) PIC code when the laser fields are zero.
4) It operates on a 2-D cartesian grid only.
5) It is parallelized via the message passing interface (MPI) and one-dimensional (1-D) domain decomposition.
6) It offers a moving window option.
7) It models tunneling ionization.

In what follows, we outline the algorithms used to realize these features and present preliminary results from the code. Further details will be presented in another paper.

II. Mathematical Description of the Algorithm

TurboWAVE is based on the proposition that the electromagnetic field can be divided into two parts: a "laser" field and a "wake" field. The laser field is characterized by two requirements. First, a typical charged particle should move through a large amount of optical phase before the field strength changes. Second, the laser energy should be confined to a small region of k-space far from the origin. The whole electromagnetic field, expressed using the normalized units typical of simulation codes, is determined by the wave equation

$$(\Delta - \partial_{tt})(\mathbf{A} + \tilde{\mathbf{a}}) = -\mathbf{J} - \tilde{\mathbf{j}} + \nabla\partial_t\phi$$

where $\tilde{\mathbf{a}}$ represents the laser component of the field and $\mathbf{A}$ represents the wake component. Correspondingly, the current density is decomposed into a rapidly varying component associated with the laser, $\tilde{\mathbf{j}}$, and a slowly varying component associated with the wake, $\mathbf{J}$. The rapidly varying current is defined as that which would be driven by the laser if the spot size was infinite

$$\tilde{\mathbf{j}} = -\tilde{\mathbf{a}}\sum_i \frac{q_i\rho_i}{m_i}.$$

Here, the sum is over the particles, ρ_i is the distribution of charge density for the ith particle, q_i is the charge, and m_i is the relativistic mass. The laser field is then defined by some initial condition, along with

$$(\Delta - \partial_{tt})\tilde{\mathbf{a}} = -\tilde{\mathbf{j}}. \tag{1}$$

Now, consider a particular component of the laser field expressed in the form

$$\tilde{a} = \frac{a(x,y,t)}{2}\, e^{i\psi} + cc$$

where $\psi = \omega(t - x)$ and ω is the laser frequency. Mora and Antonsen, Jr., showed [2] that if the radiation is dominantly forward propagating, the evolution of the laser envelope a is approximated by

$$(\Delta_T - 2i\omega\partial_\tau + 2\partial_{\tau\xi})a = -\chi a \tag{2}$$

where $\xi = x - t$, $\tau = t$, Δ_T is the transverse Laplacian, and

$$\chi = -\sum_i \frac{q_i\rho_i}{\langle m_i\rangle}$$

$$\langle m\rangle = \sqrt{m_0^2 + P^2 + \frac{q^2|a|^2}{2}}.$$

Here, m_0 is the rest mass and P is the momentum induced by the wake. Thus, the particles couple to the laser through the parameter χ, which depends on the charge density ρ and the average relativistic mass $\langle m\rangle$.

TurboWAVE models the wake fields using the same algorithm as WAVE. In particular, the potentials are updated according to

$$(\Delta - \partial_{tt})\mathbf{A} = -\mathbf{J} + \nabla\hat{G}(\nabla\cdot\mathbf{J})$$

$$\phi = -\hat{G}\rho$$

where $\hat{G}$ represents a Poisson solver. The use of $\partial_t\phi = \hat{G}(\nabla\cdot\mathbf{J})$ ensures charge conservation. The electric field $\mathbf{E}$ and magnetic field $\mathbf{B}$ are found from $\mathbf{E} = -\partial_t\mathbf{A} - \nabla\phi$ and $\mathbf{B} = \nabla\times\mathbf{A}$. The exact differencing scheme involves various subtle smoothing operations, which we will not discuss here.

The coupling between the laser and the wake takes place through the intermediary of the particles. This is expressed by the momentum equation [2]

$$\partial_t\mathbf{P} = q\left(\mathbf{E} + \mathbf{v}\times\mathbf{B} - \frac{1}{4}\frac{q}{\langle m\rangle}\nabla|a|^2\right).$$

Here, $\mathbf{E}$ and $\mathbf{B}$ are the fields associated with the wake potentials $\mathbf{A}$ and ϕ. The term involving a represents the ponderomotive force due to the laser. This expression is accurate, provided the particles move through a large number of optical cycles before the laser intensity changes significantly. Once the particle states are updated, the source terms ρ, $\mathbf{J}$, and χ can be updated. These are then used to update $\mathbf{E}$, $\mathbf{B}$, and a, so that the process can start over. Taking $a = 0$, this reduces to the usual cycle of a PIC code.

III. The Laser Field Solver

In solving numerically for the laser fields, we approximate (2), which can be written as

$$\left(1 - \frac{\partial_\xi}{i\omega}\right)\partial_\tau a = \frac{1}{2i\omega}\left(\chi a + \Delta_T a\right).$$

Multiplying both sides by $1 + \partial_\xi/i\omega$, and transforming to ordinary coordinates using $\partial_\tau = \partial_t + \partial_x$ and $\partial_\xi = \partial_x$, we obtain

$$(\partial_x + \partial_t)a = \frac{1}{2i\omega}\left(1 + \frac{\partial_x}{i\omega}\right)(\chi a + \Delta_T a) \tag{3}$$

where a term of order $1/\omega^2$ has been dropped from the left-hand side. The effect of this term is to reduce the axial group velocity of waves propagating at an angle to the axis. It can be neglected in the case of forward or near-forward Raman scattering, but could be important for Raman sidescatter.

We use Crank–Nicholson to solve (3) stably. In particular, the terms $\partial_t a$ and $\Delta_T a/2i\omega$ are evaluated using data from timesteps $n-1$ and $n+1$, whereas all other terms are evaluated at timestep n.

IV. The Pusher

TurboWAVE uses a modified version of the Boris pusher [12]. At timestep n, we regard as known r^n, $P^{n-1/2}$, ϕ^n, $A^{n-1/2}$, $A^{n+1/2}$, $a^{n-1/2}$, and $a^{n+1/2}$. This gives E^n, B^n, and $F^n = \nabla|a^n|^2$ in straightforward way. However, to advance P in a manner accurate to second order in the timestep requires knowledge of m^n. An implicit equation for m^n is

$$m^n \approx m^{n-1/2} + q\left(\mathbf{E}^n - \frac{q}{4m^n}\mathbf{F}^n\right)\cdot\frac{\mathbf{P}^{n-1/2}}{m^{n-1/2}}\frac{\Delta t}{2}$$

which can be solved using the quadratic formula. The momentum is then updated using

$$\mathbf{P}^{n+1/2} = \hat{R}\left(\mathbf{P}^{n-1/2} + \frac{\mathbf{I}}{2}\right) + \frac{\mathbf{I}}{2}$$

where

$$\mathbf{I} = \left(q\mathbf{E}^n - \frac{1}{4}\frac{q^2}{m^n}\mathbf{F}^n\right)\Delta t$$

and $\hat{R}$ is an operator that rotates a vector about the magnetic field by an angle

$$\theta = -\frac{qB^n}{m^n}\Delta t.$$

The update of the particle position is also subtle because knowledge of $m^{n+1/2}$ is required. This quantity depends implicitly on $r^{n+1/2}$ through its dependence on a. An implicit equation for $m^{n+1/2}$ is obtained by Taylor expanding $a^{n+1/2}$ about r^n

$$(m^{n+1/2})^2 = m_0^2 + (P^{n+1/2})^2 + \frac{q^2a^2}{2}$$

where

$$a^2 = [a^{n+1/2}(r^n)]^2 + \nabla[a^{n+1/2}(r^n)]^2\cdot\frac{\mathbf{P}^{n+1/2}}{m^{n+1/2}}\frac{\Delta t}{2}.$$

Again, this can be solved using the quadratic formula.

V. The Wake Field Solver

As mentioned above, the field solver for the wake is nearly identical to that of WAVE. The only difference is in the Poisson solver, where we have added the option of using open-ended boundary conditions [13]. This allows for the possibility of a nonneutral simulation box. Use of open boundary conditions is also necessary in cases in which the plasma does not fill the box transversely, such as when it is created by tunneling ionization. In such cases, neither axial boundary can be taken to be an equipotential because electron diffusion will lead to a restoring space-charge field.

VI. Moving Window

We have implemented a moving window option using a technique similar to that of PEGASUS [14]. However, in turboWAVE, boundary conditions are difficult because in the Coulomb gauge, neither $\mathbf{A}$ nor ϕ are causal quantities. A temporary solution has been to use the open boundary conditions for the Poisson solver, and to obtain a boundary condition for A_y by requiring

$$E_y = -\partial_t A_y - \partial_y\phi = 0$$

at the front of the window. The boundary condition for A_x is then found from the gauge condition

$$\partial_x A_x + \partial_y A_y = 0.$$

This technique assumes that all charges are neutralized by the time they pass through the rear boundary of the window. It is desirable, therefore, to leave a large space between the rear of the laser pulse and the rear of the window.

Although we have not yet implemented it, there is a way of rigorously computing the potentials in the moving window even for $\nabla\cdot\mathbf{A} = 0$. The method is an interesting study in causality. It accounts for sources behind the window without any knowledge of their motions. In the Appendices, we show that the effects of these sources can be expressed entirely in terms of a scalar potential ϕ_1 determined from

$$\partial_t\phi_1(\xi,k,t) = \begin{cases} -\rho_0(t)\xi/2, & k=0 \\ -k\phi_1 + \rho_0(t)e^{-k\xi}/2k, & k\neq 0. \end{cases} \quad (4)$$

Here, a Fourier transform has been performed in the y-direction, k is the Fourier wavenumber, $\xi = x - t$ is a coordinate moving with the window, and ρ_0 is the charge density at the rear boundary of the window ($\xi = 0$). The total scalar potential is then $\phi_1 + \phi$, where ϕ is computed assuming $\rho = 0$ outside the window.

An alternative solution is to rewrite the field solver to operate in the Lorentz gauge. In particular, we could solve

$$(\Delta - \partial_{tt})\mathbf{A} = -\mathbf{J} + \nabla\hat{G}(\partial_t\rho + \nabla\cdot\mathbf{J})$$
$$(\Delta - \partial_{tt})\phi = -\rho.$$

Here, again, the Poisson solver $\hat{G}$ is used to ensure charge conservation. Although $\hat{G}$ is not a causal operator, the vector potential will be very nearly causal nevertheless. This is because for a linearly weighted $\mathbf{J}$, the contribution of a particle to $(\partial_t\rho + \nabla\cdot\mathbf{J})$ takes the form of a quadrupole. The resulting "correction field" is therefore highly localized to the region of the particle [13]. With both potentials causal, the moving window boundary conditions can be done as in PEGASUS.

VII. Ionization

In many laser–plasma interaction experiments, the plasma is created by the laser via tunneling ionization. It is desirable therefore to include this process in any laser–plasma simulation code. Tunneling ionization is modeled in turboWAVE by computing an ionization rate based on the Keldysh model [15]. This rate is computed in each grid cell to determine the number of new particles to create in that cell. The particles are given a thermal

velocity selected by the user and can be positioned either uniformly or randomly throughout the cell.

VIII. Parallelization

Parallelization of turboWAVE is accomplished using the (MPI). One-dimensional domain decomposition is done in the x-direction. This is largely straightforward, except for the Poisson solver. The WAVE Poisson solver works by transforming to frequency space in the y-direction and finite differencing in the x-direction. The operation in the y-direction parallelizes immediately because it is independent of x. After this transformation, the scalar potential at each y is determined from a second-order difference equation in x. Because the domain decomposition is performed in the x-direction, solution of this equation requires a parallel tridiagonal solver. We have devised and implemented such an algorithm. It is presented in the Appendices.

IX. Benchmarking

We have tested turboWAVE by modeling phenomena that can be described analytically, and by comparing it with fully explicit calculations done using WAVE and PEGASUS. We treat these benchmarks in order of increasing complexity.

A. Vacuum Propagation

The simplest test is to verify that the laser field solver correctly propagates a Gaussian beam in vacuum. In slab geometry, a Gaussian beam is described by

$$a(x,y,t) = a_0 \frac{w_0}{\sqrt{w_0 w}}\, e^{-y^2/w^2} e^{-i\psi}$$

where

$$w = w_0\sqrt{1+\frac{x^2}{x_R^2}}$$
$$\psi = \frac{1}{2}\tan^{-1}\frac{x}{x_R} - \frac{wy^2}{2R}$$
$$R = x\left(1+\frac{x_R^2}{x^2}\right)$$

and the Rayleigh length is

$$x_R = \tfrac{1}{2}\omega w_0^2.$$

As a test, we focus a laser pulse to the center of a simulation box $2.67x_R$ long. This is done simply by setting the amplitude and phase of a in the left ghost cell according to $a(-1.33x_R, y, t)$. Fig. 1(a) shows the resulting transverse amplitude profile in the center of the box. The vertical dotted lines show the locations of $\pm w_0$, and the horizontal dotted line shows the location of a_0/e. The curve passes through the intersections of these lines just as expected.

Fig. 1(b) shows the relative phase of a on axis. A "Guoy phase shift" of $\pi/4$ radians is expected as the laser propagates through $2x_R$. This is exactly what is observed.

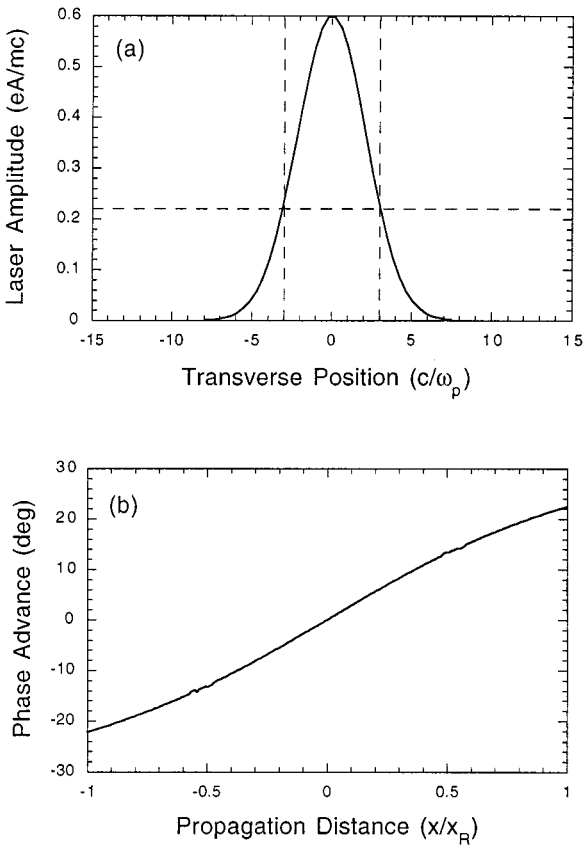

Fig. 1. Test of propagation in vacuum (a) amplitude profile at best focus. The curve is expected to pass through the intersections of the dotted lines (b) Guoy phase shift. The phase shift through one Rayleigh length is expected to be 22.5°.

B. Linear Propagation in Plasma

For the next test, we propagate a small amplitude wave through a uniform plasma in one dimension. Let

$$\tilde{a} = e^{i\omega(t-x)}e^{i\phi(x)} = e^{i(\omega t - kx)}$$

where ϕ is the phase change due to plasma. It follows that $k = \omega - \phi/x$. Assuming the plasma is homogeneous, it further follows that $\phi = mx$, where m is constant. Using the well-known dispersion relation for electromagnetic waves in a plasma, we obtain

$$m = \omega - \sqrt{\omega^2 - \omega_p^2}.$$

In Fig. 2, we plot $\phi(x)$ for an electromagnetic wave with $\omega = 10$ propagating through a box with a vacuum region and a plasma region. The slope of the curve corresponds to m. As expected, the slope is zero in the vacuum region and ≈ 0.05 in the plasma region.

C. Beat Excitation of a Plasma Wave

It was shown by Rosenbluth and Liu [16] that a two-frequency laser will drive a plasma wave such that the electrostatic field grows according to

$$\frac{E_x(t)}{E_0} = \frac{a_1 a_2}{4}\,\omega_p t$$

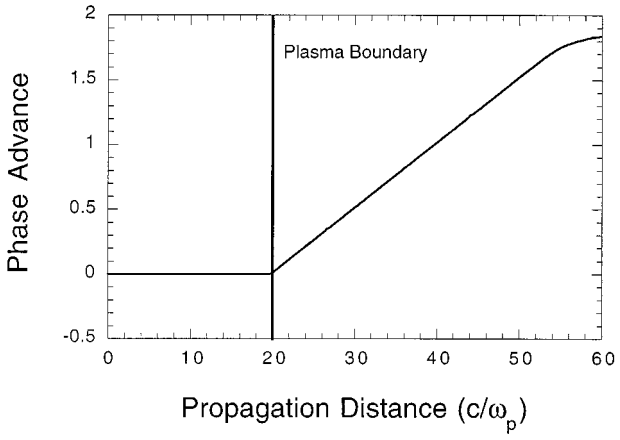

Fig. 2. Linear propagation in a plasma for $\omega = 10\omega_p$. The slope of the curve corresponds to $c(k_{\rm vac} - k)/\omega_p$. The expected slope in the plasma region is 0.05, just as is observed in the plot.

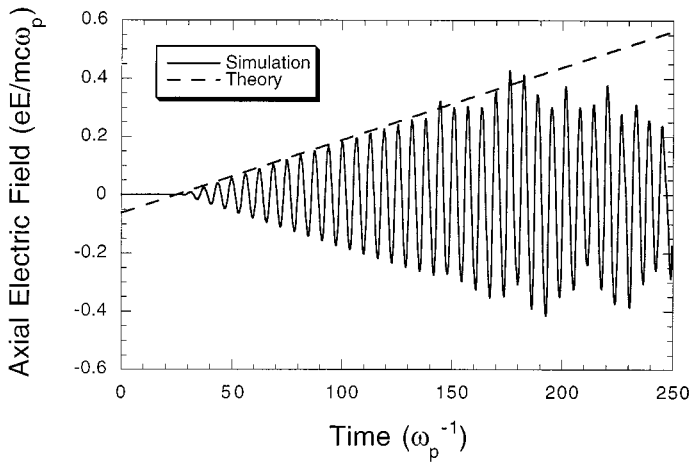

Fig. 3. Beat excitation of a plasma wave with $a_1 = a_2 = 0.1$, $\omega_1 = 9.5$, and $\omega_2 = 10.5$. The electric field grows secularly at the expected rate until relativistic detuning occurs.

where E_0 is the cold wavebreaking field, a_1 and a_2 are the normalized amplitudes of the two lasers, and the frequencies of the two lasers are chosen such that $\omega_1 - \omega_2 = \omega_p$. Fig. 3 shows the results of a 1-D simulation in which $a_1 = a_2 = 0.1$ and $(\omega_1 + \omega_2)/2 = 10\omega_p$. A particular point in the simulation box was chosen, and $E_x(t)$ was plotted. The field grows linearly at the expected rate until relativistic detuning saturates it.

D. Wakefield Excitation

In the (1-D) nonrelativistic limit, the amplitude of the wake excited by a short pulse laser is [6]

$$\phi = \frac{1}{4}\int_0^{\zeta} |a(\zeta')|^2 \sin(\zeta - \zeta')\, d\zeta' \tag{5}$$

where $\zeta = x - t$. We test the accuracy of this in both one and two dimensions, using both the moving and stationary windows. The temporal profiles of the pulses used are of the form

$$f(t) = \begin{cases} 10\tau^3 - 15\tau^4 + 6\tau^5, & 0 < t < t_w \\ 10\xi^3 - 15\xi^4 + 6\xi^5, & t_w < t < 2t_w \end{cases}$$

where $\tau = t/t_w$, $\xi = 2 - t/t_w$, and t_w is the full-width at half-maximum (FWHM) of the pulse. The function f has the following properties: $f(0) = f(2t_w) = 0$, $f(t_w) = 1$, $f(t_w/2) = f(3t_w/2) = 1/2$, $f'(0) = f'(t_w) = f'(2t_w) = 0$, and $f''(0) = f''(t_w/2) = f''(t_w) = f''(3t_w/2) = f''(2t_w) = 0$.

Fig. 4(a) shows the results of both 1-D and 2-D simulations in which the wake amplitude ϕ was measured as a function of the driver amplitude a. The 2-D simulations used the moving window. The laser parameters were $\omega = 20$ and $t_w = 3.0$. For the 2-D runs, the spot size was $w_0 = 3.0$. The theoretical curve was obtained by numerically integrating (5). The agreement between theory and simulation is excellent for small a. For large a, relativistic effects are expected to reduce the wake amplitude from the theoretical value, as is indeed observed in the figure.

Fig. 4(b) shows the results of 1-D simulations in which the wake amplitude ϕ was measured as a function of the pulse length t_w. The laser amplitude was $a = 0.4$, and the frequency was

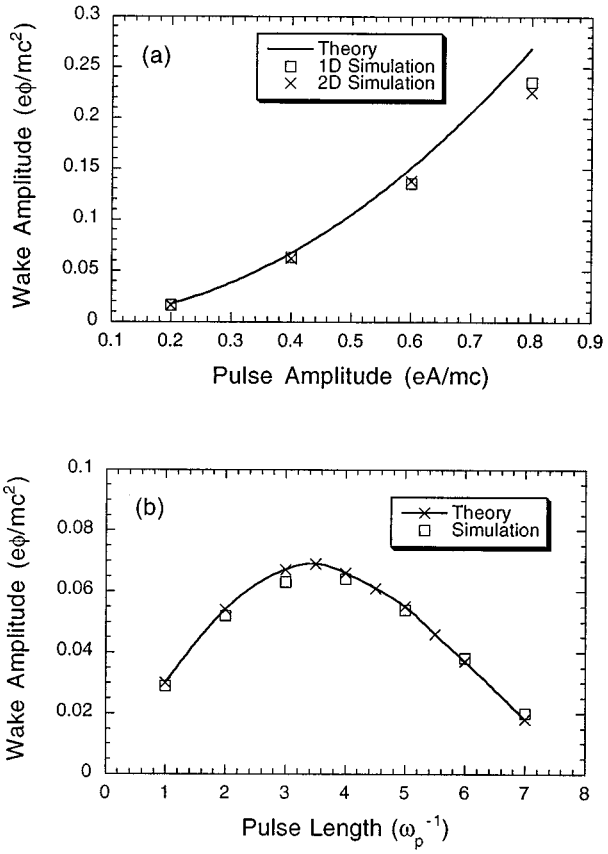

Fig. 4. Excitation of wakes by a short-pulse (a) scaling with driver amplitude and (b) scaling with pulse length near the resonance.

$\omega = 20$. The theoretical curve was again obtained by numerically integrating (5). Again, the agreement between theory and simulation is excellent.

E. Nonlinear Beat Excitation

In [17], a fully explicit 2-D simulation of beat excitation was done using WAVE, in which $a_1 = a_2 = 0.56$, $\omega_1 = 4\omega_p$, and $\omega_2 = 5\omega_p$. The laser risetime was $\omega_p t = 300$. Late during this risetime, the wave amplitudes become large enough so that no

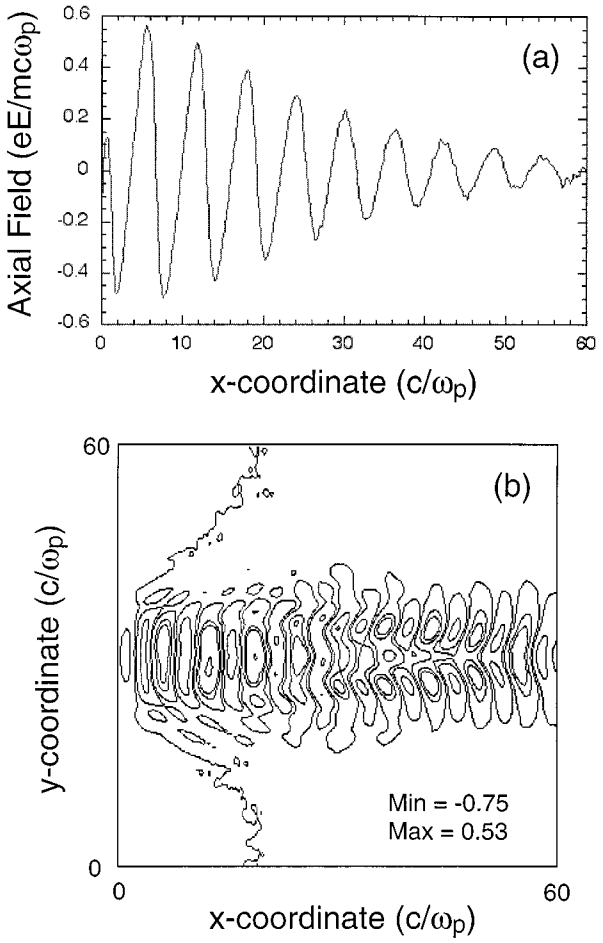

Fig. 5. Nonlinear beat excitation (a) axial electric field at $\omega_p t = 150$ and (b) scalar potential at $\omega_p t = 210$.

analytical treatment is available. To test how well turboWAVE works under such conditions, we repeat the simulation described in [17] using the ponderomotive guiding center algorithm.

Fig. 5(a) shows the on-axis axial electric field at at a time shortly before the waves become highly nonlinear. This corresponds to [17, Fig. 12(b)]. The agreement is excellent. Fig. 5(b) shows a contour plot of the scalar potential after a high degree of nonlinearity has set in. This corresponds to [17, Fig. 15(c)]. The similarity between the two sets of contours is striking.

F. Self Modulation

Finally, we consider the case of the self-modulation of a short pulse propagating through a plasma. This is a difficult problem to model using a ponderomotive guiding center code for two reasons. First, it has been shown [18], [14] that backscatter can strongly affect the outcome of such an interaction. This is because the Raman backscatter instability grows very quickly and acts as a seed for the forward Raman instability and self-modulation. In regimes in which this seeding mechanism dominates, its absence from the model causes the forward Raman to develop much more slowly than it should and the entire interaction can end up looking very different. The second difficulty is that the forward Raman leads to wavebreaking and the generation of large numbers of very high-energy electrons. These

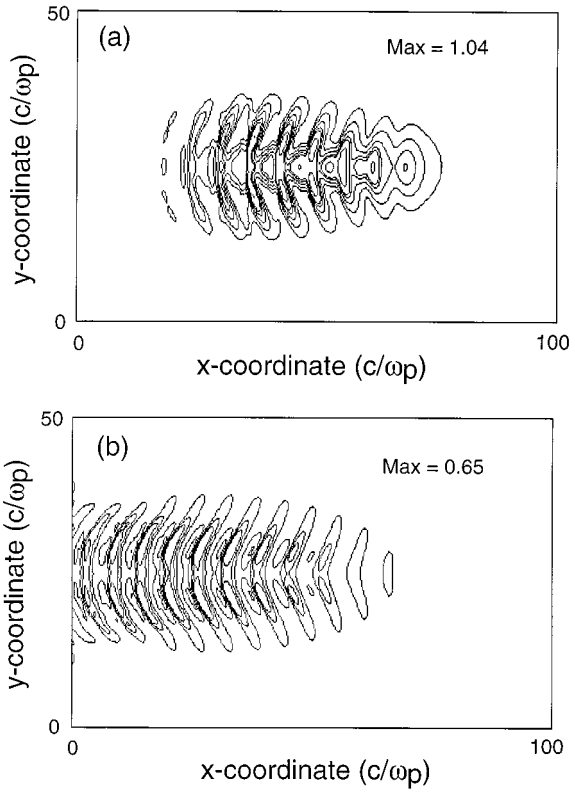

Fig. 6. Self modulation of a short-pulse (a) laser amplitude at $\omega_p t = 150$, including seed pulse and (b) accelerating electric field at $\omega_p t = 150$.

electrons may move too slowly through the optical phase fronts to be modeled accurately by the ponderomotive description.

Despite the difficulties described above, we have found that it is possible to obtain reasonable results in the self-modulated regime using turboWAVE. At sufficiently early times, the incorrect interaction between the high-energy electrons and the laser fields is not expected to strongly affect the evolution of the laser or the wake because the number of high-energy electrons is small. The backscatter problem is not serious, provided the wake driven by the rising edge of the laser pulse is sufficiently strong. In particular, if the wake is strong enough to seed the forward Raman as strongly and as quickly as backscatter, backscatter will not have a serious impact on the interaction. This is because once the forward instabilities are underway, they dominate over all other processes.

As an example that illustrates these difficulties, and how to overcome them, we attempt to reproduce the 2-D PEGASUS simulation described in [18]. Unfortunately, [18] describes the pulse shape in terms of a parameter $l_0 = 50c/\omega_p$ which is not precisely defined. We choose to interpret this parameter in the sense that makes the problem as challenging as possible—that is, we take the pulse shape to be as described in Section IX-D with $t_w = l_0$. Other parameters were $a_0 = 0.75$, $\omega = 5$, and $w_0 = 9$. In this case, the wake excited by the rising edge of the pulse takes much longer to excite the forward Raman than does backscatter. However, we find that the effects of backscatter can be simulated by superimposing a small short pulse $(t_w = \pi)$ over the longer main pulse. This takes the place of the "notch" that backscatter would have created in the laser pulse via pump

depletion. Using this technique along with the moving window, we generated Fig. 6. The contours of laser amplitude at $\omega_p t = 150$ are shown in Fig. 6(a), whereas the contours of the axial electric field at the same time are shown in Fig. 6(b). These are to be compared respectively with [18, Figs. 3(c) and (d)]. The two sets of results are qualitatively similar. Better quantitative agreement might be obtained by adjusting the seed pulse. It should also be noted that the need for a seed pulse might be eliminated given a more favorable interpretation of l_0. We indeed ran a case with a different pulse shape (equal risetime, fall-time, and flat-top regions of $30\omega_p^{-1}$) and found that contours similar to those shown in Fig. 6 could be generated without a seed pulse.

X. Conclusion

The code turboWAVE provides an effective method of modeling laser–plasma interactions, in which the laser radiation is dominantly forward propagating and the laser–particle interaction is adequately modeled by the ponderomotive force. Plans for the future include implementation of cylindrical geometry and three dimensions, as well as the improved moving window algorithm discussed above. In addition, a method of handling high-energy particles whose interaction with the laser is not adequately modeled by the ponderomotive force is being contemplated.

Appendix A
Moving Window Poisson Solver

To solve for $\mathbf{A}$ and ϕ in a computational region, or "window," moving at the speed of light, requires a Poisson solver that accounts for sources behind the window without knowing what those sources are. The key to solving this problem lies in understanding the implications of causality. By causality, the fields in the window are independent of the sources behind the window. This means particles behind the window can undergo any motion whatsoever without affecting the solution for the fields in the window. The problem then is to choose some motion that makes it easy to solve for the potentials. The obvious choice is to immediately "freeze" the particles the moment they cross the rear boundary of the window. The particles then recede from the window at the speed of light while maintaining their transverse position.

The equations for the potentials can be written as follows:

$$(\Delta - \partial_{tt})\mathbf{A} = -\mathbf{J} + \nabla G * (\nabla \cdot \mathbf{J})$$
$$\phi = -G * \rho.$$

Here, G is a Green's function and $*$ represents convolution in space. If we choose to freeze the particles the moment they cross the rear boundary of the window, the current behind the window is zero and the sources behind the window do not contribute to the vector potential. To solve for the scalar potential due to sources behind the window, we Fourier transform in the transverse direction. This gives

$$\phi(x,k,t) = -\int_{-\infty}^{t} G(x-x',k)\rho(x',k,t)\,dx'$$

where for $k \neq 0$

$$G(x,k) = -\frac{1}{2k}\,e^{-k|x|}.$$

The upper limit in the integral $x = t$ is the location of the rear boundary of the window. Because the sources behind the window do not move, we have for $x < t$

$$\rho(x,t) = \rho(x,x) = \rho_0(x)$$

where $\rho_0(x)$ is the charge density on the boundary evaluated at the time $t = x$. This allows the convolution integral to be written as

$$\phi = \frac{e^{-kx}}{2k}\int_{-\infty}^{t} e^{kt'}\rho_0(t')\,dt'$$

where we renamed the integration variable to emphasize that the integration is effectively over time. In terms of a coordinate $\xi = x - t$ moving with the window, this becomes

$$\phi(\xi,k,t) = \frac{e^{-k(\xi+t)}}{2k}\int_{-\infty}^{t} e^{kt'}\rho_0(t')\,dt'$$

Differentiating both sides with respect to time gives (4). The solution for the $k = 0$ mode is found similarly, using for the Green's function

$$G(x,k=0) = \frac{|x|}{2}.$$

Appendix B
Parallel Tridiagonal Solver

We seek a parallelizable solution to the equation

$$A_{ji}\phi_i = -\rho_j$$

where A is a tridiagonal matrix. Consider $L+1$ diagonal submatrices of size $N \times N$ defined by

$$A^n_{ji} = A_{j+nN,i+nN}$$

where n varies from 0 to L and i, j vary from 1 to N. From the original matrix equation, it follows that

$$A^n\phi^n = -\rho^n - \theta^n\phi_N^{n-1}\mathbf{b}_1 - \eta^n\phi_1^{n+1}\mathbf{b}_N$$

where $\mathbf{b}_i$ are the standard basis vectors and

$$\theta^n = A_{nN+1,nN}$$
$$\eta^n = A_{nN+N,nN+N+1}.$$

Inverting this equation gives

$$\phi^n = \psi^n - \alpha^n\mathbf{v}^n - \beta^n\mathbf{w}^n \tag{6}$$

where

$$\alpha^n = \phi_N^{n-1} = \phi_0^n$$
$$\beta^n = \phi_1^{n+1} = \phi_{N+1}^n$$
$$\psi^n = -(A^n)^{-1}\rho^n$$
$$\mathbf{v}^n = \theta^n(A^n)^{-1}\mathbf{b}_1$$
$$\mathbf{w}^n = \eta^n(A^n)^{-1}\mathbf{b}_N.$$

Let us now regard n as indicating one of the nodes on a parallel computer. The quantities ψ, $\mathbf{v}$, and $\mathbf{w}$ can be solved for inde-

pendently on each node via the usual tridiagonal algorithm. To obtain the full solution ϕ, it only remains to solve for α^n and β^n.

The quantities α^n and β^n can be viewed as the dirichlet boundary conditions to the left and right of node n, respectively. Equation (6) can, therefore, be viewed as expressing the solution on a single node in terms of the solution ψ using null boundary conditions, plus a correction taking into account the actual boundary conditions imposed by the presence of the other nodes. These boundary conditions are determined implicitly by combining the definitions of α^n and β^n with (6). In particular, we have $2L$ equations

$$\alpha^n = \psi_N^{n-1} - k_1^{n-1}\alpha^{n-1} - k_2^{n-1}\beta^{n-1}$$
$$\beta^n = \psi_1^{n+1} - k_3^{n+1}\alpha^{n+1} - k_4^{n+1}\beta^{n+1}$$

for the $2L$ unknowns $\alpha^1 \cdots \alpha^L$ and $\beta^0 \cdots \beta^{L-1}$. Here

$$k_1^n = v_N^n$$
$$k_2^n = w_N^n$$
$$k_3^n = v_1^n$$
$$k_4^n = w_1^n.$$

The system is closed by taking α^0 and β^L as given. These can be viewed as the dirichlet boundary conditions for the whole system. Alternatively, if the global boundary conditions are accounted for by the original equation $A\phi = -\rho$, then $\alpha^0 = \beta^L = 0$.

The above system of equations can be reexpressed in terms of two independent tridiagonal systems: one for α^n and one for β^n. In particular

$$a^n\alpha^{n-1} + b^n\alpha^n + c^n\alpha^{n+1} = s^n, \qquad n = \{1 \cdots L\}$$
$$x^n\beta^{n-1} + y^n\beta^n + z^n\beta^{n+1} = r^n, \qquad n = \{0 \cdots L-1\}$$

where for the α system, we have

$$s^n = \psi_N^{n-1} - k_2^{n-1}\psi_1^n + \left(k_2^{n-1}/k_2^n\right)k_4^n\psi_N^n$$
$$a^n = k_1^{n-1}$$
$$b^n = 1 - k_2^{n-1}k_3^n + \left(k_2^{n-1}/k_2^n\right)k_1^n k_4^n$$
$$c^n = \frac{k_2^{n-1}}{k_2^n}\,k_4^n$$
$$\alpha^{L+1} = \psi_N^L - k_1^L\alpha^L - k_2^L\beta^L$$

and for the β system, we have

$$r^n = \psi_1^{n+1} - k_3^{n+1}\psi_N^n + \left(k_3^{n+1}/k_3^n\right)k_1^n\psi_1^n$$
$$x^n = \frac{k_3^{n+1}}{k_3^n}\,k_1^n$$
$$y^n = 1 - k_2^n k_3^{n+1} + \left(k_3^{n+1}/k_3^n\right)k_1^n k_4^n$$
$$z^n = k_4^{n+1}$$
$$\beta^{-1} = \psi_1^0 - k_3^0\alpha^0 - k_4^0\beta^0.$$

The α^n factors can be computed on one node—the "alpha node"—whereas the β^n factors are computed on another—the "beta node." Once this is done, the alpha node transmits α^n to node n while the beta node transmits β^n to node n. Node n can then compute ϕ^n, and the problem is solved.

In many cases, the system $A\phi = -\rho$ has to be solved repeatedly under conditions in which ρ changes but A does not. In this case, certain quantities can be computed on the first pass through the program's main loop,whereas subsequent iterations reuse the results of that calculation. These quantities are $\mathbf{v}$, $\mathbf{w}$, k_1 through k_4, a, b, c, x, y, and z.

The message passing requirements for the algorithm just described are as follows. For each tridiagonal system to be solved, six numbers must be passed from every node to the alpha node. The same six numbers must be passed from every node to the beta node. These numbers are ψ_1, ψ_N, and k_1 through k_4. The alpha and beta nodes then operate on these parameters to produce L correction factors each. Finally, the alpha node sends one number to each node ($\alpha^n \rightarrow$ node n), while the beta node does likewise.

One way to improve the efficiency of the message passing is to write the routine in such a way that it handles multiple tridiagonal systems at a time. For example, one might have a 2-D grid on which a tridiagonal solution is required over each horizontal strip. In this case, it would be best to pass the ψ and k factors for every strip in one message. This alleviates the problem of latency.

REFERENCES

[1] P. Mora and T. M. Antonsen, "Electron cavitation and acceleration in the wake of an ultra-intense, self focused laser pulse," *Phys. Rev. E*, vol. 53, p. 2068, 1996.

[2] ——, "Kinetic modeling of intense, short laser pulses propagating in tenuous plasmas," *Phys. Plasmas*, vol. 4, p. 217, 1997.

[3] D. W. Forslund, J. M. Kindel, and E. L. Lindman, "Theory of stimulated scattering processes in laser-irradiated plasmas," *Phys. Fluids*, vol. 18, no. 8, pp. 1002–1016, Aug. 1975.

[4] K. Estabrook and W. L. Kruer, "Theory and simulation of one-dimensional Raman backward and forward scattering," *Phys. Fluids*, vol. 26, no. 7, pp. 1892–1903, July 1983.

[5] M. Tabak, J. Hammer, M. E. Glinsky, W. L. Kruer, S. C. Wilks, J. Woodworth, E. M. Campbell, M. D. Perry, and R. J. Mason, "Ignition and high gain with ultrapowerful lasers," *Phys. Plasmas*, vol. 1, p. 1626, 1994.

[6] E. Esaray, P. Sprangle, J. Krall, and A. Ting, "Overview of plasma-based accelerator concepts," *IEEE Trans. Plasma Sci.*, vol. 24, p. 252, 1996.

[7] W. B. Mori, "Special issue on generation of coherent radiation using plasmas," *IEEE Trans. Plasma Sci.*, vol. 21, 1993.

[8] N. H. Burnett and G. D. Enright, "Population inversion in the recombination of optically-ionized plasmas," *IEEE J. Quantum Electron.*, vol. 26, p. 1797, 1990.

[9] A. Lal, D. Gordon, K. Wharton, C. E. Clayton, K. A. Marsh, W. B. Mori, C. Joshi, M. J. Everett, and T. W. Johnston, "Spatio-temporal dynamics of the resonantly excited relativistic plasma wave driven by a CO_2 laser," *Phys. Plasmas*, vol. 4, p. 1434, 1997.

[10] P. Sprangle, E. Esarey, and A. Ting, "Nonlinear theory of intense laser-plasma interactions," *Phys. Rev. Lett.*, vol. 64, p. 2011, 1990.

[11] R. L. Morse and C. W. Nielson, "Numerical simulation of the Weibel instability in one and two dimensions," *Phys. Fluids*, vol. 14, no. 4, p. 830, Apr. 1971.

[12] J. P. Boris, "Relativistic plasma simulation-optimization of a hybrid code," presented at the Proc. 4th Conf. Numer. Simul. Plasmas, 1970.

[13] C. K. Birdsall and A. B. Langdon, *Plasma Physics via Computer Simulation*, Bristol, U.K.: IOP, 1991.

[14] K. C. Tzeng, W. B. Mori, and C. D. Decker, "Anomalous absorption and scattering of short-pulse high-intensity lasers in underdense plasmas," *Phys. Rev. Lett.*, vol. 76, p. 3332, 1996.

[15] L. V. Keldysh, "Ionization in the field of a strong electromagnetic wave," *Soviet Phys. JETP*, vol. 20, no. 5, pp. 1307–1314, May 1965.

[16] M. N. Rosenbluth and C. S. Liu, "Excitation of plasma waves by two laser beams," *Phys. Rev. Lett.*, vol. 29, pp. 701–705, Sept. 1972.

[17] W. B. Mori, "Theory and simulations on beat wave excitation of relativistic plasma waves," Ph.D. dissertation, University of California, Los Angeles, CA, 1987.

[18] C. Decker, W. B. Mori, and T. Katsouleas, "Particle-in-cell simulations of Raman forward scattering from short-pulse high-intensity lasers," *Phys. Rev. E*, vol. 50, p. 3338, 1994.

Daniel F. Gordon, received the B.S., M.S., and Ph.D. degrees in electrical engineering from the University of California, Los Angeles, in 1991, 1995, and 1999, respectively.

He is currently a National Research Council research associate at the Naval Research Laboratory, Washington, DC. His research interests are in high intensity, short pulse, laser-plasma interactions, plasma based accelerators, and computer modeling.

W. B. Mori, photograph and biography not available at the time of publication.

Thomas M. Antonsen, Jr. (M'87) was born in Hackensack, NJ, in 1950. He received the B.S. degree in electrical engineering in 1973, and the M.S. and Ph.D. degrees in 1976 and 1977, all from Cornell University, Ithaca, NY.

He was a National Research Council Post Doctoral Fellow at the Naval Research Laboratory in 1976–1977, and a Research Scientist in the Research Laboratory of Electronics at MIT from 1977 to 1980. In 1980, he moved to the University of Maryland where he joined the faculty of the Departments of Electrical Engineering and Physics in 1984. He is currently a Professor of physics and electrical engineering. He has held visiting appointments at the Institute for Theoretical Physics (UCSB), the Ecole Polytechnique Federale de Lausanne, Switzerland, and the Institute de Physique Theorique, Ecole Polytechnique, Palaiseau, France. His research interests include the theory of magnetically confined plasmas, the theory and design of high power sources of coherent radiation, nonlinear dynamics in fluids, and the theory of the interaction of intense laser pulses and plasmas. He is the author and coauthor of more than 180 journal articles and coauthor of the book *Principles of Free-electron Lasers*. He has served on the editorial board of *Physical Review Letters*, *The Physics of Fluids*, and *Comments on Plasma Physics*.

Prof. Antonsen was selected as a Fellow of the Division of Plasma Physics of the American Physical Society in 1986.